

Nonequilibrium dynamics of a mixed spin-1/2 and spin-3/2 Ising ferrimagnetic system with a time dependent oscillating magnetic field source

Erol Vatansever

Dokuz Eylül University, Graduate School of Natural and Applied Sciences, TR-35160 Izmir, Turkey

Hamza Polat*

Department of Physics, Dokuz Eylül University, TR-35160 Izmir, Turkey

(Dated: June 14, 2018)

Nonequilibrium phase transition properties of a mixed Ising ferrimagnetic model consisting of spin-1/2 and spin-3/2 on a square lattice under the existence of a time dependent oscillating magnetic field have been investigated by making use of Monte Carlo simulations with single-spin flip Metropolis algorithm. A complete picture of dynamic phase boundary and magnetization profiles have been illustrated and the conditions of a dynamic compensation behavior have been discussed in detail. According to our simulation results, the considered system does not point out a dynamic compensation behavior, when it only includes the nearest-neighbor interaction, single-ion anisotropy and an oscillating magnetic field source. As the next-nearest-neighbor interaction between the spins-1/2 takes into account and exceeds a characteristic value which sensitively depends upon values of single-ion anisotropy and only of amplitude of external magnetic field, a dynamic compensation behavior occurs in the system. Finally, it is reported that it has not been found any evidence of dynamically first-order phase transition between dynamically ordered and disordered phases, which conflicts with the recently published molecular field investigation, for a wide range of selected system parameters.

I. INTRODUCTION

The phenomenon of ferrimagnetism is related to the counteraction of opposite magnetic moments with unequal magnitudes located on different sublattices. Ferrimagnetic materials have, under certain conditions, a compensation temperature at which the resultant magnetization vanishes below its critical temperature¹. Recently, it has been both experimentally and theoretically shown that the coercive field exhibits a rapid increase at the compensation point^{2,3}. It is obvious that such kind of point has a technological importance^{4,5}, because at this point only a small driving field is required to change the sign of the resultant magnetization. Due to the recent developments in experimental techniques, scientists begin to synthesize new classes of molecular-based magnets⁶⁻⁸. For instance, it has been shown that the saturation magnetization, chemical analysis and infrared spectrum analysis of $V(TCNE)_{x,y}(\text{solvent})$, where TCNE is tetracyanoethylene, are consistent with a ferrimagnet with spin-3/2 at the vanadium site and a spin of 1/2 at the TCNE sites with $x \sim 2^7$. In this regard, it is possible to mention that the theoretical models referring the mixed systems are of great importance since they are well adopted to study and to provide deeper understanding of certain type of ferrimagnetism¹.

From the theoretical point of view, a great deal number of studies have been realized to get a clear idea about the magnetic properties of mixed spin-1/2 and spin-3/2 ferrimagnetic Ising systems. In order to have a general overview about it, it is beneficial to classify the studies in two categories based on the investigation of equilibrium and nonequilibrium phase transition properties of such type of mixed spin systems. In the former group, static or equilibrium properties of these type of systems have been analyzed within the several frameworks such as exact^{9,10}, effective field theory with correlations¹¹⁻²², Bethe lattice²³⁻²⁶, exact star-triangle mapping transformation²⁷, high temperature series expansion method²⁹, multisublattice Green-function technique³⁰, Oguchi approximation³¹ as well as Monte Carlo simulation³². It is underlined in the some studies noted above that when the system includes only the nearest-neighbor interaction between spins and the single-ion anisotropy, the temperature variation of resultant magnetization does not exhibit a compensation behavior. In contrary to this, when the next-nearest neighbor interaction between spins-1/2 takes into account and exceeds a minimum value which depends upon the other system parameters, the ferrimagnetic system reveals a compensation treatment which can not be observed in single-spin Ising systems.

Magnetically interacting system under the influence of a magnetic field varying sinusoidally in time exhibits two important striking phenomena: Nonequilibrium phase transitions and dynamic hysteresis behavior. Nowadays, these types of nonequilibrium systems are in the center of scientists because they have exotic, unusual and interesting behaviors. For example, the universality classes of the Ising model and its variations under a time dependent driving field are different from its equilibrium counterparts³³⁻³⁵. It is possible to emphasize that nonequilibrium phase transitions originate due to a competition between time scales of the relaxation time of the system and oscillating period of the external applied field. For the high temperatures and high amplitudes of the periodically varying magnetic field, the simple kinetic ferromagnetic system exists in dynamically disordered phase where the time dependent

magnetization oscillates around value of zero and is able to follow the external applied magnetic field with some delay, whereas it oscillates around a non-zero value which indicates a dynamically ordered phase for low temperatures and small magnetic field amplitudes³⁶. The physical mechanism described briefly above points out the existence of a dynamic phase transition (DPT)^{33,36,37}.

DPTs and hysteresis behaviors can also be observed experimentally. For example, by benefiting from surface magneto-optic Kerr effect (MOKE), dynamic scaling of magnetic hysteresis in ultrathin ferromagnetic Fe/Au(001) films has been studied, and it is reported that the dispersion of hysteresis loop area of studied system obeys to a power law behavior³⁸. A comprehensive study, which includes the hysteresis loop measurement of well-characterized ultrathin Fe films grown on flat and stepped W(110) surfaces, has been done by using MOKE, and prominent experimental observations are reported in Ref.³⁹. In addition to these pioneering works mentioned briefly above, to the best of our knowledge, there exist a number of experimental studies regarding the nonequilibrium properties of different types of magnetic materials such as Co films on a Cu(001) surface⁴⁰, polycrystalline Ni₈₀Fe₂₀ films⁴¹, epitaxial Fe/GaAs(001) thin films⁴², Fe_{0.42}Zn_{0.58}F₂⁴³, finemet thin films with composition Fe_{73.5}Cu₁Nb₃Si_{13.5}B₉⁴⁴, [Co/Pt]₃ magnetic multilayers with strong perpendicular anisotropy⁴⁵ as well as assembly of paramagnetic colloids⁴⁶. Based upon the detailed experimental investigations, it has been discovered that experimental nonequilibrium dynamics of considered real magnetic systems strongly resemble the dynamic behavior predicted from theoretical calculations of a kinetic Ising model. From this point of view, it is possible to see that there exists an impressive evidence of qualitative consistency between theoretical and experimental investigations.

On the other hand, in the latter group there exists a limited number of nonequilibrium studies concerning the influences of time varying magnetic field on the mixed spin-1/2 and spin-3/2 Ising ferrimagnetic model. For instance, thermal and magnetic properties of a mixed Ising ferrimagnetic model consisting of spin-1/2 and spin-3/2 on a square lattice have been analyzed by making use of Glauber-type stochastic process⁴⁷. It has been reported that the studied system always exhibits a dynamic tricritical point in amplitude of external applied field and temperature plane, but it does not show in the single-ion anisotropy and temperature plane for low values of amplitude of field⁴⁸. Following the same methodology, a similar study has been done to shed some light on what happens when an oscillating magnetic field is applied to the mixed spin-1/2 and spin-3/2 Ising model on alternate layers of hexagonal lattice. It has been found that depending on the Hamiltonian parameters, the system presents dynamic multicritical as well as compensation behaviors⁴⁹. However, the aforementioned studies are mainly based on molecular field theory. It is a well known fact that, in molecular field theory, spin fluctuations are ignored and the obtained results do not have any microscopic information details of system. From this point view, in order to obtain the true dynamics of a mixed spin-1/2 and spin-3/2 Ising ferrimagnetic system on a square lattice under the presence of a time dependent oscillating magnetic field, we intend to use of Monte Carlo simulation technique which takes into account the thermal fluctuations, and in this way, non-artificial results can be obtained.

The outline of the paper is as follows: In section II we briefly present our model. Section III is dedicated to the results and discussion, and finally section IV contains our conclusions.

II. FORMULATION

We consider a two-dimensional kinetic Ising ferrimagnetic system with mixed spins of $\sigma = 1/2$ and $S = 3/2$ defined on a square lattice, and the system is exposed to a time dependent magnetic field source. The Hamiltonian describing our model is given by

$$\mathcal{H} = -J_1 \sum_{\langle nn \rangle} \sigma_i^A S_j^B - J_2 \sum_{\langle nnn \rangle} \sigma_i^A \sigma_k^A - D \sum_j (S_j^B)^2 - H(t) \left(\sum_i \sigma_i^A + \sum_j S_j^B \right) \quad (1)$$

where the $\sigma_i = \pm 1/2$, and $S_j = \pm 3/2, \pm 1/2$ are the Ising spins on the sites of the sublattices A and B, respectively. First and second sums in Eq. (1) are over the nearest- and next-nearest neighbor pairs of spins, respectively. We assume $J_1 < 0$ such that the exchange interaction between nearest neighbours is antiferromagnetic. J_2 is the exchange interaction parameter between pairs of next-nearest neighbors of spins located on sublattice A, and D is single ion-anisotropy term which affects only $S = 3/2$ spins located on sublattice B. The time varying sinusoidal magnetic field is as following

$$H(t) = h_0 \sin(\omega t) \quad (2)$$

here, h_0 and ω are amplitude and angular frequency of the external field, respectively. The period of the oscillating magnetic field is given by $\tau = 2\pi/\omega$.

The linear dimension of the lattice is selected as $L = 40$ through all simulations, and Monte Carlo simulation based on Metropolis algorithm⁵⁰ is applied to the kinetic mixed Ising ferrimagnetic system on a 40×40 square lattice with periodic boundary conditions in all directions. Configurations were generated by selecting the sites sequentially through the lattice and making single-spin-flip attempts, which were accepted or rejected according to the Metropolis algorithm. Data were generated over 50 independent samples realizations by running the simulations for 60000 MC steps per site after discarding the first 20000 steps. This amount of transient steps is found to be sufficient for thermalization for the whole range of the parameter sets. Error bars are found by using Jackknife method⁵¹. Because the calculated errors are usually smaller than the sizes of the symbols in the obtained figures, they have not been given in this study.

The instantaneous values of the sublattice magnetizations M_A and M_B , and also the total magnetization M_T at the time t are defined as

$$M_A(t) = \frac{2}{L^2} \sum_{i \in A} \sigma_i^A, \quad M_B(t) = \frac{2}{L^2} \sum_{j \in B} S_j^B, \quad M_T(t) = \frac{M_A(t) + M_B(t)}{2}. \quad (3)$$

By benefiting from the instantaneous magnetizations over a full period of oscillating magnetic field, we obtain the dynamic order parameters as follows

$$Q_A = \frac{1}{\tau} \oint M_A(t) dt, \quad Q_B = \frac{1}{\tau} \oint M_B(t) dt, \quad Q_t = \frac{1}{\tau} \oint M_T(t) dt, \quad (4)$$

where Q_A , Q_B and Q_t denote the dynamic order parameters corresponding to the sublattices A and B , and the overall lattice, respectively. To determine the dynamic compensation temperature T_{comp} from the computed magnetization data, the intersection point of the absolute values of the dynamic sublattice magnetizations was found using

$$|Q_A(T_{comp})| = |Q_B(T_{comp})|, \quad (5)$$

$$\text{sign}(Q_A(T_{comp})) = -\text{sign}(Q_B(T_{comp})), \quad (6)$$

with $T_{comp} < T_c$, where T_c is the dynamic critical temperature. We also calculate the time average of the cooperative part of energy of the kinetic mixed Ising ferrimagnetic system over a full cycle of the magnetic field as follow⁵²

$$E_{coop} = -\frac{1}{L^2 \tau} \oint \left(J_1 \sum_{\langle nn \rangle} \sigma_i^A S_j^B + J_2 \sum_{\langle nnn \rangle} \sigma_i^A \sigma_k^A + D \sum_j (S_j^B)^2 \right) dt. \quad (7)$$

Thus, the specific heat of the system is defined as

$$C_{coop} = \frac{E_{coop}}{dT}, \quad (8)$$

where T represents the temperature. We should mention here that DPT points separating the dynamically ordered and disordered phases are determined by benefiting from the peaks of heat capacities. We also verified that the peak positions of heat capacities do not significantly alter when larger L is selected.

III. RESULTS AND DISCUSSION

In this section, we will focus our attention on the nonequilibrium dynamics of the mixed spin-1/2 and spin-3/2 Ising ferrimagnetic system under a time dependent magnetic field. First of all, we will discuss the dynamic nature of the system when the system includes only the nearest-neighbor interaction between spins, the single-ion anisotropy and external applied field. Next, we will give and argue the global dynamic phase diagrams including the both dynamic critical and compensation temperatures in the case of the existence the next-nearest neighbor interaction between spins-1/2 located on sublattice A. Before we discuss the DPT features of the considered system, we should notice that the situation of $h_0/|J_1| = 0.0$ indicates the equilibrium case, and our Monte Carlo simulation findings for this value of $h_0/|J_1|$ are completely in accordance with the recently published work³² where the equilibrium properties of the present system were analyzed by following a numerical methodology of heat-bath Monte Carlo algorithm.

The considered system exhibits three types of magnetic behaviors depending on the Hamiltonian parameters. These are dynamically ferrimagnetic (*i*), ferromagnetic (*f*) and paramagnetic (*p*) phases, respectively. In the first type of phase, namely in *i* phase, $|Q_A| \neq |Q_B|$, and, the time dependent sublattice magnetizations, $M_A(t)$ and $M_B(t)$ oscillate with time around a non-zero value whereas they alternate around a non-zero value and $|Q_A| = |Q_B|$ in the second type of phase, namely in *f* phase. In *p* phase which corresponds to the third type of phase, $|Q_A| = |Q_B|$ and $M_A(t)$ and $M_B(t)$ oscillate around zero value, and they are delayed with respect to the external applied magnetic field. Keeping in this mind, we illustrate the dynamic phase diagrams in a $(D/|J_1| - k_B T_c/|J_1|)$ plane with three oscillation periods $\tau = 50, 100$ and 200 and for some selected values of the applied field amplitudes ($h_0/|J_1|$) in Figs. 1(a)-(c). One of the main findings is that DPT temperature decreases as the value of applied field amplitude increases. The physical mechanism underlying this observation can be much better understood by following a simple way: If one keeps the system in one well of a Landau type double well potential, a certain amount of energy coming from magnetic field is necessary to achieve a dynamic symmetry breaking. If the amplitude of the applied field is less than the required amount then the system oscillates in one well. In this situation, the magnetization does not change its sign. In other words, the system oscillates around a non-zero value corresponding to a dynamically ordered phase. As the temperature increases, the height of the barrier between the two wells decreases. As a result of this, the less amount of magnetic field is necessary to push the system from one well to another and hence the magnetization can change its sign for this amount of magnetic field. Consequently, the time averaged magnetization over a full cycle of the oscillating magnetic field becomes zero. For the relatively high oscillation period values, dynamic magnetizations corresponding to the instantaneous sublattice order parameters can respond to the oscillating magnetic field with some delay, whereas a competition occurs between the period τ of the field and the relaxation time of the system as the period of the external magnetic field decreases. Hence, the dynamic magnetizations can not respond to the external magnetic field due to the increasing phase lag between the field and the time dependent magnetization. This mechanism makes the occurrence of the DPT difficult for the considered system. Another important observation is that an unexpected sharp dip occurs between dynamically ordered and disordered phases in the $(D/|J_1| - k_B T_c/|J_1|)$ plane with increasing value of the amplitude of the external applied field, and our results show that observation such kind of treatment explicitly depends upon the value of τ of field. Furthermore, it is necessary to state that for both large negative and positive values of single-ion anisotropies, the phase transition points saturate a certain temperature regions, and they tend to shift to the lower temperature regions with increasing amplitude and period of the external applied field.

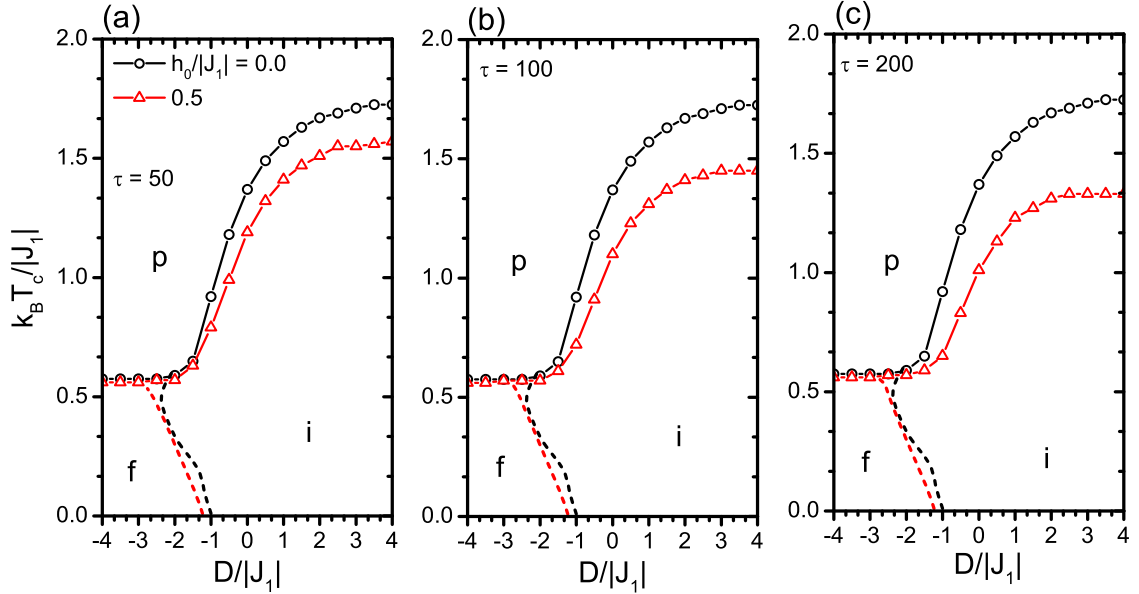


FIG. 1: (Color online) Dynamic phase boundaries of the system in the $(D/|J_1| - k_B T_c/|J_1|)$ plane with some selected values of external field amplitudes $h_0/|J_1| = 0.0$ and 0.5 . The curves are plotted for three values of oscillating period: (a) $\tau = 50$, (b) $\tau = 100$ and (c) $\tau = 200$. The dotted lines are boundary lines between two dynamically ordered phases.

In Figs. 2(a)-(b), we depict the effect of the single-ion anisotropy on the thermal variations of dynamic order parameters corresponding to the phase diagram illustrated in Fig. 1(a) for value of $h_0/|J_1| = 0.5$. It is clear from the figures that the treatments of the thermal variations of sublattices as well as total magnetizations curves sensitively depend upon the value of single-ion anisotropy, for selected values of Hamiltonian parameters. In the

bulk ferrimagnetism of Néel, it is possible to classify the thermal variation of the total magnetization curve in certain categories¹. According to this nomenclature, for $D/|J_1| \geq 0$, the considered system clearly points out a Q-type behavior, where the magnetizations of system begin to decrease gradually starting from their saturation values with increasing thermal agitation, and then they vanish at the DPT point. One can easily see that, in the range $-1 < D/|J_1| < 0$, the magnetizations tend to fall prominently from their saturation values, and the system undergoes a second order DPT as temperature increases. In addition to these, when $D/|J_1| < -1$, the system exhibits a L-type behavior at which the total magnetization shows a temperature induced maximum which definitively depends on the value of single-ion anisotropy as well as other Hamiltonian parameters. Based on the above simulation observations, it is possible to make an inference that the studied system has three types of dynamic magnetic behavior. It is also worthy of note that even though the magnitudes of spins are different from each other, both Q_A and Q_B exhibit a DPT at the same critical temperature, which is a result of the nearest-neighbor exchange coupling J_1 .

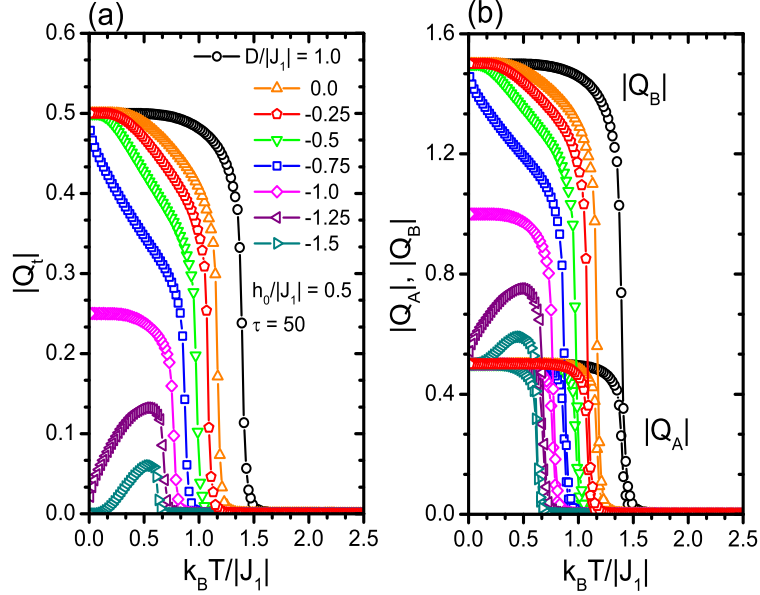


FIG. 2: (Color online) Effects of the single-ion anisotropy on the thermal variations of order parameters $|Q_t|$, $|Q_A|$ and $|Q_B|$ for a combination of Hamiltonian parameters corresponding to the phase diagram depicted in Fig. 1.

The influences of the applied field amplitude $h_0/|J_1|$ on the thermal variations of total and sublattice magnetizations as well as dynamic heat capacity of the system are plotted in Figs. 3(a)-(c) corresponding to the phase diagram constructed in Fig. 1(a) with value of single-ion anisotropy $D/|J_1| = 1.0$. In Fig. 3(a), total magnetization curves of the system are shown. As seen in this figure, magnetization curves exhibit Q-type behavior and dynamic critical temperatures decreases with increasing $h_0/|J_1|$ values. On the other hand, dynamic heat capacity curves which are depicted in Fig. 3(c) show a sharp peak behavior indicating the phase transition temperature. Moreover, one can readily see that increasing value of the applied field amplitude gives rise to decrease the maximum of the dynamic heat capacity curves. We should note here that such kinds of dynamic heat capacity behaviors have been found in a ferrimagnetic core-shell nanoparticle composed of a spin-3/2 ferromagnetic core which is surrounded by a spin-1 ferromagnetic shell layer under the presence of a time dependent magnetic field^{53,54}.

In Fig. 4, we investigate the effect of the applied field period on the DPT features of the system. Phase diagrams in Fig. 4(a) are constructed for a value of the applied field amplitude $h_0/|J_1| = 0.5$. It is possible to say that DPT points are depressed with increasing applied field period especially in the high values of the single-ion anisotropy. The physics behind of these findings are identical to those emphasized in Fig. 1. Therefore, we will not discuss these interpretations here. Instead of this, in Fig. 4(b) we will give the influence of applied field period on the thermal variations of sublattice magnetizations for a considered value of single-ion anisotropy $D/|J_1| = 1.0$ corresponding to the phase diagram illustrated in Fig. 4(a). It is found that as the thermal agitation increases starting from zero, the values of sublattice magnetizations begin to gradually decrease and the system undergoes a DPT at the critical temperature which sensitively depends on value of the τ .

According to our simulation results, the kinetic mixed spin-1/2 and spin-3/2 Ising ferrimagnetic system including only nearest-neighbor interaction between spins, the single-ion anisotropy and external applied field does not display a dynamic multicritical behavior for a wide range of Hamiltonian parameters used in here, in contrary to the previously

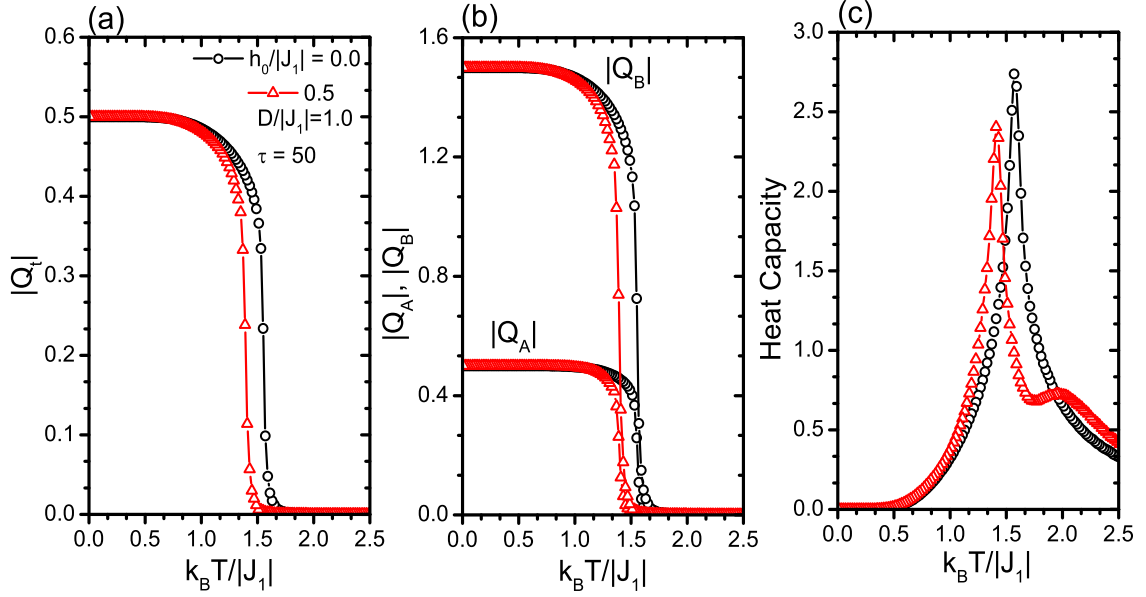


FIG. 3: (Color online) Temperature dependencies of (a) total magnetization $|Q_t|$, (b) sublattice magnetizations $|Q_A|$ and $|Q_B|$, and (c) dynamic heat capacity for $D/|J_1| = 1.0$ and $\tau = 50$ with $h_0/|J_1| = 0.0$ and 0.5 .

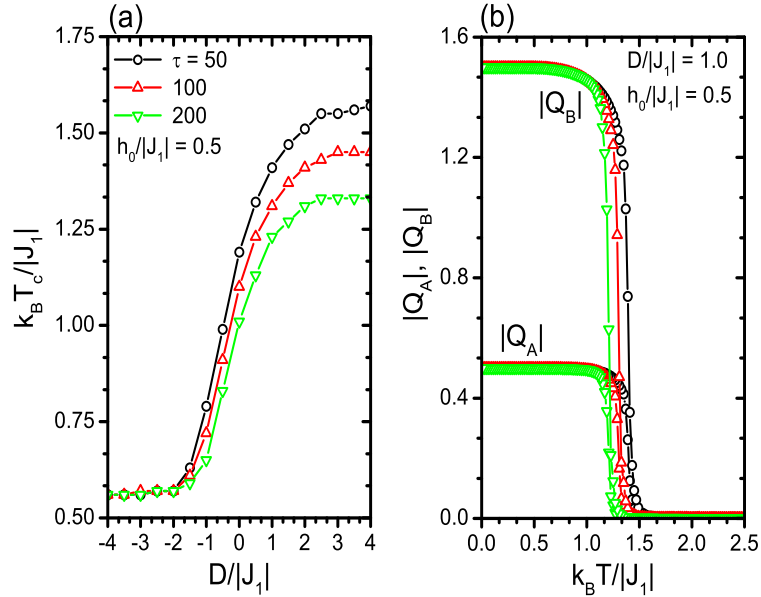


FIG. 4: (Color online) (a) Dynamic phase boundaries of the system in $(D/|J_1| - k_B T_c/|J_1|)$ plane for $h_0/|J_1| = 0.5$ with $\tau = 50, 100$ and 200 . (b) Effects of the external applied field period on the thermal variations of sublattice magnetizations $|Q_A|$ and $|Q_B|$ for $D/|J_1| = 1.0$ and $\tau = 50, 100$ and 200 .

published molecular field investigation where dynamic first order phase transitions and dynamic tricritical points have been reported for the same model⁴⁸.

In the following analysis, in order to shed some light on the effect of the next-nearest neighbor interaction between spins-1/2 of the studied system, we give the dynamic phase boundaries in $(J_2/|J_1| - k_B T/|J_1|)$ plane for some considered values of applied field amplitudes with $\tau = 100$ in Figs. 5(a-c). The phase boundaries containing both dynamic critical and compensation temperatures are plotted for three values of single-ion anisotropies $D/|J_1| = -1.0, 0.0$ and 1.0 , respectively. At first sight, one can clearly see that the dynamic compensation temperatures do not emerge until $J_2/|J_1|$ reaches a certain amount of value. After the aforementioned value of $J_2/|J_1|$, with an increment in $J_2/|J_1|$ does not lead to change the location of dynamic compensation point for fixed values of $D/|J_1|$ and $h_0/|J_1|$.

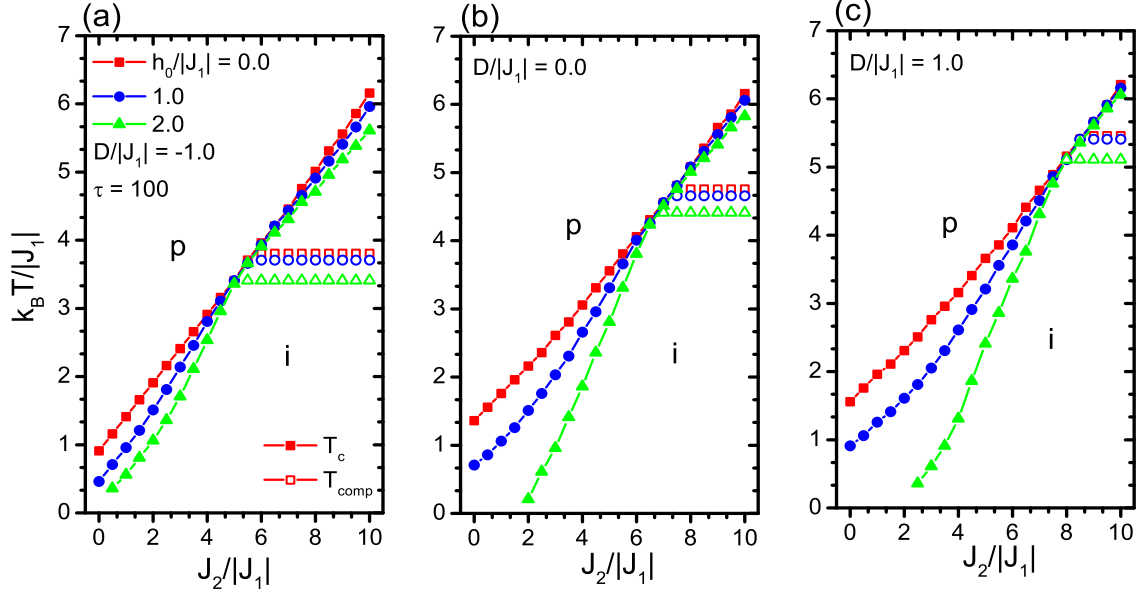


FIG. 5: (Color online) Dynamic phase boundaries including both critical and compensation temperatures in $(J_2/|J_1| - k_B T/|J_1|)$ plane for $\tau = 100$ and with some selected values of external field amplitudes $h_0/|J_1| = 0.0, 1.0$, and 2.0 . The curves are plotted for three values of single-ion anisotropies (a) $D/|J_1| = -1.0$, (b) $D/|J_1| = 0.0$ and (c) $D/|J_1| = 1.0$.

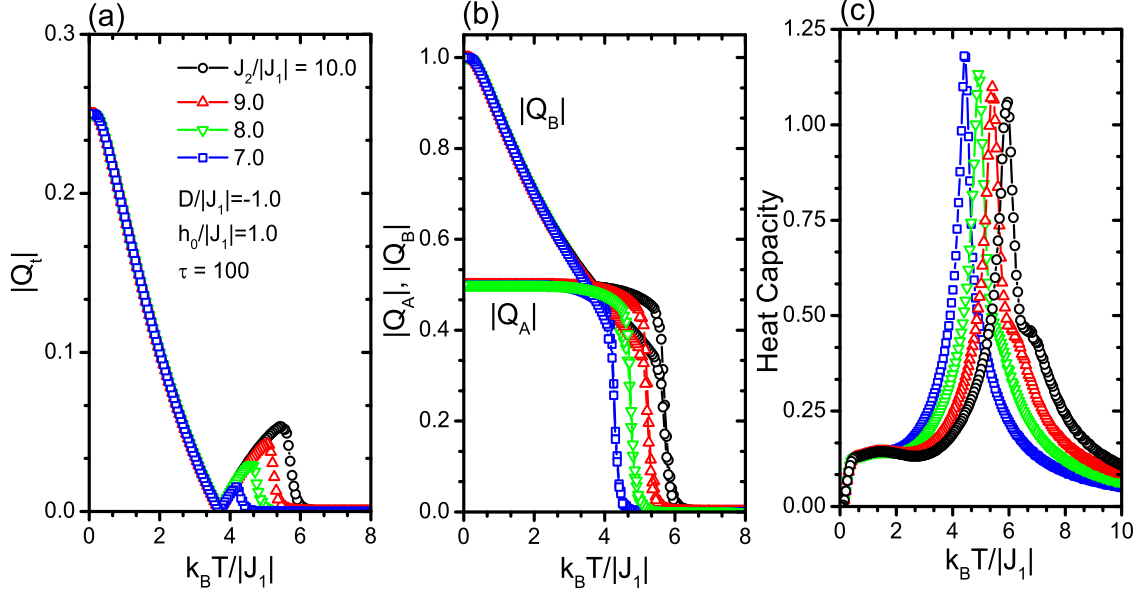


FIG. 6: (Color online) Influences of the next-nearest neighbor interactions on the thermal variations of (a) total magnetization $|Q_t|$, (b) sublattice magnetizations $|Q_A|$ and $|Q_B|$ and (c) dynamic heat capacity for some selected values of Hamiltonian parameters corresponding to the phase diagram illustrated in Fig. 5.

In contrary to this behavior, in accordance with the expectations, as the value of $J_2/|J_1|$ gets bigger starting from zero, the much more thermal energy is necessary to reveal a DPT. On the other side, both the dynamic critical and compensation temperatures strongly depend upon the selected values of $D/|J_1|$ and $h_0/|J_1|$. An increase in the value of $h_0/|J_1|$ gives rise to shift the dynamic critical and compensation points to lower temperatures and also allows the system to display a dynamic compensation behavior at the relatively low value of $J_2/|J_1|$. Additionally, it is possible to make an inference that with increasing value of single-ion anisotropy, the region where the dynamic compensation behavior occurs shifts to upward for considered Hamiltonian parameters. This situation can be well understood by comparing the Figs. 5(a), (b) and (c) with each other.

Effects of the next-nearest neighbor interactions on the thermal variations of total and sublattice magnetizations as well as on dynamic heat capacity of the studied system for some selected values of $D/|J_1| = -1.0$, $h_0/|J_1| = 1.0$ with $\tau = 100$ corresponding to the phase diagram shown in Fig. 5(a) are seen in Figs. 6(a-c). We give the total magnetization curves for changing value of $J_2/|J_1|$ in Fig. 6(a). These curves explicitly refer the existence of a dynamic compensation behaviors, and they also exhibit a N-type magnetic behavior. As we discussed before, varying value of $J_2/|J_1|$ does not give rise to cause a change in value of dynamic compensation point in temperature plane. Besides, in order to show how the dynamic compensation phenomenon rises, thermal variations of the absolute values of sublattice magnetizations are given in Fig. 6(b). It can be said that an increase in value of $J_2/|J_1|$ leads to the existence of a dynamically stronger ferromagnetic interaction between σ spins. In this way, the σ spins can remain ordered at relatively higher temperatures. When the thermal energy increases starting from zero, the values of sublattice magnetizations begin to gradually decrease from their saturation values until both sublattices magnetizations are equal in magnitude at a certain temperatures at which dynamic compensation point emerges below the dynamic critical transition temperature. $J_2/|J_1|$ dependencies of dynamic heat capacities are presented in Fig. 6(c). It is obvious from the figure that the dynamic heat capacity curves exhibit a sharp peak at the transition temperature, and when the value of $J_2/|J_1|$ increases, the dynamically ordered phase region gets wider, in other words, the location of the sharp peak slides to a higher value in the temperature plane. The shape of the heat capacity curves are also nearly same for selected values of Hamiltonian parameters.

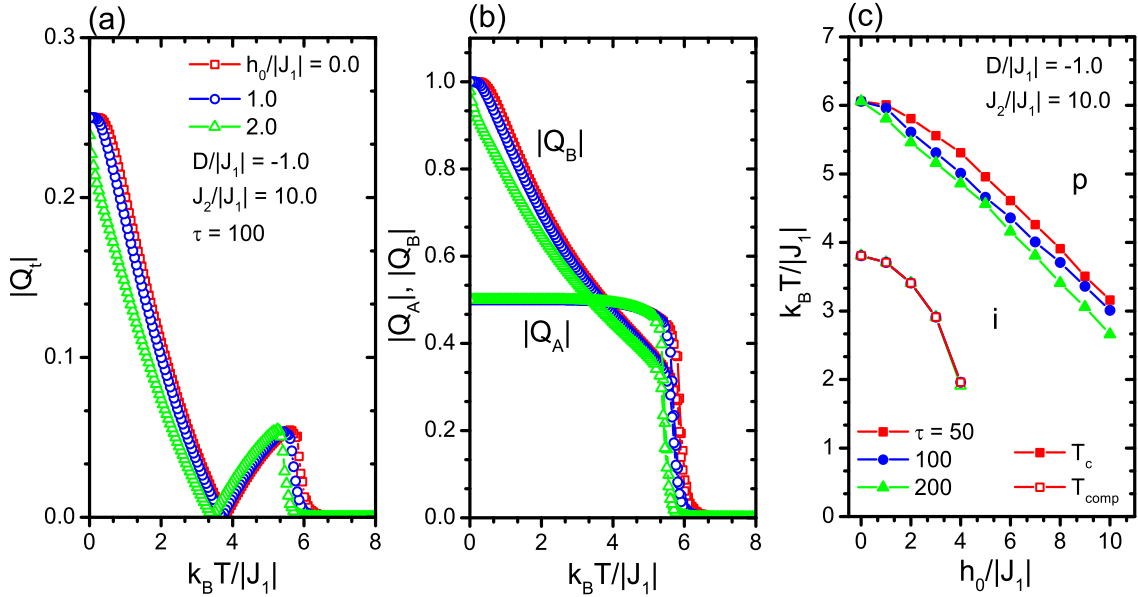


FIG. 7: (Color online) Effects of external applied field amplitude on the thermal variations of order parameters $|Q_t|$, $|Q_A|$ and $|Q_B|$ for $D/|J_1| = -1.0$, $J_2/|J_1| = 10.0$ and $\tau = 100$ with $h_0/|J_1| = 0.0, 1.0$ and 2.0 .

As a final investigation, we give and discuss the influences of varying value of applied field amplitude on the thermal variations of total and sublattices magnetizations exhibiting dynamic compensation as well as critical temperatures in Figs. 7(a-b) corresponding to the dynamic phase boundary seen in Fig. 5(a) for $J_2/|J_1| = 10.0$. It is possible to mention that both dynamic compensation and critical temperatures strongly depend on value of the external applied field amplitude and they tend to shift to a lower region in temperature plane, and compensation behavior disappears with increasing value of $h_0/|J_1|$. In order to demonstrate the detailed magnetic behavior of system, we give the dynamic phase boundaries in $(h_0/|J_1| - k_B T/|J_1|)$ planes for three values of the applied field periods such as $\tau = 50, 100$ and 200 for selected values of single-ion anisotropy $D/|J_1| = -1.0$ and next-nearest neighbor interaction $J_2/|J_1| = 10.0$ in Fig. 7(c). Based on the calculated phase diagrams, it can be said that the decreasing (increasing) applied field period has no effect on the dynamic behavior of compensation behavior whereas it affects prominently the dynamic critical temperature of the system such that the dynamically ordered phase region gets wider (narrower).

IV. CONCLUDING REMARKS

In conclusion, it has been carried out a detailed Monte Carlo investigation based on standard single-spin flip Metropolis algorithm to determine the true DPT properties of a mixed spin-1/2 and spin-3/2 Ising ferrimagnetic system under a time varying magnetic field. A complete picture of global dynamic phase diagrams separating the dynamically disordered and ordered phases has been constructed by benefiting from the peaks of thermal variations of dynamic heat capacities in order to have a better understanding of the physical background underlying of the considered system. The most important observations reported in the present study can be briefly summarized as follows:

- When the considered system only includes the nearest-neighbor interaction, single-ion anisotropy and a time dependent sinusoidally oscillating magnetic field, it does not point out a dynamic compensation point.
- Stationary state solutions of the system strongly depend on the selected system parameters. As discussed in detail in previous section, with increasing values of amplitude and period of the external applied field, the dynamic phase boundaries tend to shift to the lower temperature regions in related planes, and a sharp dip occurs between dynamically ordered and disordered phases.
- In contrary to the previously published investigation for the same model where dynamic first-order phase transitions and tricritical points have been reported⁴⁸, it has not been found any evidence of the dynamic first-order phase transitions in our present work. The reason is most likely the fact that the method we used completely takes into account the thermal fluctuations, which allows us to obtain non-artificial results.
- When the next-nearest neighbor interaction between spins-1/2 is included and exceeded a characteristic value which sensitively depends on value of the single-ion anisotropy and amplitude of the external applied field, the system exhibits a dynamic compensation behavior below its critical temperature. According to the our simulation results, the changing value of applied field period has no effect on the location of dynamic compensation point.

Finally, we should note that it is possible to improve the obtained results by making use of a more realistic system such as Heisenberg type of Hamiltonian. From the theoretical point of view, such an interesting problem may be subject of a future work in order to provide deeper understanding of ferrimagnetic materials under a time dependent alternating magnetic field source.

Acknowledgements

The numerical calculations reported in this paper were performed at TÜBİTAK ULAKBİM (Turkish agency), High Performance and Grid Computing Center (TRUBA Resources).

-
- * Electronic address: hamza.polat@deu.edu.tr
- ¹ L. Néel, Ann. Phys. (Paris) **3**, 137 (1948).
 - ² P. Hansen, J. Appl. Phys. **62**, 216 (1987).
 - ³ G.M. Buendia, and E. Machado, Phys. Rev. B **61**, 14686 (2000).
 - ⁴ M. Mansuripur, J. Appl. Phys. **61**, 1580 (1987).
 - ⁵ H.-P.D. Shieh, and M.H. Kryder, Appl. Phys. Lett. **49**, 473 (1986).
 - ⁶ J.M. Manriquez, G.T. Yee, R.S. McLean, A.J. Epstein, and J.S. Miller, Science **252**, 1415 (1991).
 - ⁷ B.G. Morin, P. Zhou, C. Hahn, and A.J. Epstein, J. Appl. Phys. **73**, 5648 (1993).
 - ⁸ G. Du, J. Joo, and A.J. Epstein, J. Appl. Phys. **73**, 6566 (1993).
 - ⁹ C. Domb, Adv. Phys. **9**, 149 (1960).
 - ¹⁰ L. L. Gonçalves, Phys. Scr. **32**, 248 (1985).
 - ¹¹ T. Kaneyoshi, M. Jaščur and P. Tomczak, J. Phys.: Condens. Matter **4**, L653 (1992); **5**, 5331 (1993).
 - ¹² T. Kaneyoshi, Physica A **215**, 378 (1995).
 - ¹³ N. Benayad, A. Dakhama, A. Klümper and J. Zittartz, Ann. Physik **5**, 387 (1996).
 - ¹⁴ A. Bobák, and M. Jurčisin, J. Magn. Mang. Mater. **163**, 292 (1996).
 - ¹⁵ A. Bobák, and D. Horváth, Phys. Stat. Sol. B **213**, 459 (1999).
 - ¹⁶ W. Jiang, G.-O. Wei, and Z.-H. Xin, Physica A **293**, 455 (2001).
 - ¹⁷ Y.-Q. Liang, G.-Z. Wei, and G.-L. Song, Phys. Stat. Sol. B **241**, 1916 (2004).

- ¹⁸ M. Aouzi, M. El Hafidi, and E.M. Sakhaf, *Physica A* **345**, 575 (2005).
- ¹⁹ I. Essaoudi, K. Bärner, A. Ainane, and M. Saber, *Physica A* **385**, 208 (2007).
- ²⁰ Y.-Q. Liang, G.-Z. Wei, X.-J. Xu and G.-L. Song, *Comm. Theor. Phys.* **53**, 957 (2010).
- ²¹ A. Yigit, and E. Albayrak, *J. Magn. Magn. Mater.* **329**, 125 (2013).
- ²² A. Yigit, and E. Albayrak, *J. Magn. Magn. Mater.* **392**, 4216 (2013).
- ²³ C. Ekiz, *J. Magn. Magn. Mater.* **293**, 913 (2005).
- ²⁴ C. Ekiz, *Physica A* **353**, 286 (2005).
- ²⁵ E. Albayrak, and A. Alci, *Physica A* **345**, 48 (2005).
- ²⁶ E. Albayrak, *Chin. Phys. B* **21**, 067501 (2012).
- ²⁷ M. Jaščur, and J. Strečka, *Physica A* **358**, 393 (2005).
- ²⁸ R.G. Bowers, and B.Y. Yousif, *Phys. Lett. A* **96**, 49 (1983).
- ²⁹ G.J.A. Hunter, R.C.L. Jenkins, and C.J. Tinsley, *J. Phys. A: Math. Gen.* **23**, 4547 (1990).
- ³⁰ J. Li, G. Wei, and A. Du, *J. Magn. Magn. Mater.* **269**, 410 (2004).
- ³¹ A. Bobák, Z. Fecková, and M. Zukovic, *J. Magn. Magn. Mater.* **323**, 813 (2011).
- ³² G.M. Buendia, and R. Cardona, *Phys. Rev. B* **59**, 6784 (1999).
- ³³ B.K. Chakrabarti, M. Acharyya, *Rev. Mod. Phys.* **71**, 847 (1999).
- ³⁴ M. Acharyya, *Int. J. Mod. Phys. C* **16**, 1631 (2005).
- ³⁵ H. Park, M. Pleimling, *Phys. Rev. Lett.* **109**, 175703 (2012).
- ³⁶ T. Tomé, M.J. de Oliveira, *Phys. Rev. A* **41**, 4251 (1990).
- ³⁷ W.S. Lo, R.A. Pelcovits, *Phys. Rev. A* **42**, 7471 (1990).
- ³⁸ Y.-L. He and G.-C. Wang, *Phys. Rev. Lett.* **70**, 2336 (1993).
- ³⁹ J.S. Suen and J.L. Erskine, *Phys. Rev. Lett.* **78**, 3567 (1997).
- ⁴⁰ Q. Jiang, H.-N. Yang, and G.-C. Wang, *Phys. Rev. B* **52**, 14911 (1995).
- ⁴¹ B.C. Choi, W.Y. Lee, A. Samad, and J.A.C. Bland, *Phys. Rev. B* **60**, 11906 (1999).
- ⁴² W.Y. Lee, B.-Ch. Choi, Y.B. Xu, and J.A.C. Bland, *Phys. Rev. B* **60**, 10216 (1999).
- ⁴³ A. Rosales-Rivera, J.M. Ferreira, and F.C. Montenegro, *J. Magn. Magn. Mater.* **226-230**, 1309 (2001).
- ⁴⁴ L. Santi, R.L. Sommer, A. Magni, G. Durin, F. Colaiori, and S. Zapperi, *IEEE Trans. Mag.* **39**, 2666 (2003).
- ⁴⁵ D.T. Robb, Y.H. Xu, O. Hellwig, J. McCord, A. Berger, M.A. Novotny, and P.A. Rikvold, *Phys. Rev. B* **78**, 134422 (2008).
- ⁴⁶ P. Tierno, T.H. Johansen, and J.M. Sancho, *Phys. Rev. E* **87**, 062301 (2013).
- ⁴⁷ R.J. Glauber, *J. Math. Phys.* **4**, 294 (1963).
- ⁴⁸ B. Deviren, M. Keskin, and O. Canko, *J. Magn. Magn. Mater.* **321**, 458 (2009).
- ⁴⁹ M. Keskin, B. Deviren and O. Canko, *IEEE Trans. Mag.* **45**, 2640 (2009).
- ⁵⁰ K. Binder, *Monte Carlo Methods in Statistical Physics* (Springer, Berlin, 1979).
- ⁵¹ M.E.J. Newman and G.T. Barkema, *Monte Carlo Methods in Statistical Physics* (Clarendon Press, Oxford 2001).
- ⁵² M. Acharyya, *Phys. Rev. E* **56**, 2407 (1997).
- ⁵³ Y. Yüksel, E. Vatansever, and H. Polat, *J. Phys.: Condens. Matter* **24**, 436004 (2012).
- ⁵⁴ E. Vatansever, and H. Polat, *J. Magn. Magn. Mater.* **343**, 221 (2013).